dilute solution. For a solution approximately 1×10^{-5} M in $Co(py)_4Cl_2^+$ and approximately 1×10^{-4} M in linpen, the disappearance of $Co(py)_4Cl_2^+$ is first order with a half-life of 48 s. When the same concentrations are maintained and approximately 2×10^{-6} M $Co(H_2O)_6^{2+}$ is added, the half-life falls to 24 s. Thus, as with the reaction with $EDTA^{4-}$ above, electron transfer is indicated as the pathway for rapid complex formation.

The efficiency of these complex formation reactions is indicated by the following preparation. When 0.25 g of $[Co(py)_4Cl_2]NO_3$ (0.0005 mol) in 50 mL of H_2O is allowed to react with 0.20 g of diethylenetriamine, dien (0.002 mol), in 10 mL of H_2O, an immediate color change to yellow is observed. Cation exchange of the product solution on a column of SP-Sephadex by elution with 0.05 M Na_3PO_4 separates the $Co(dien)_2^{3+}$ product into its three geometric isomers.[16] The total yield of the three isomers was near 100% based upon title complex used, and no other Co(III) species were observed. Furthermore, the isomer distribution (*s-fac*:*u-fac*:*mer*) was far from the equilibrium isomer distribution as indicated in Table I. The increase in the proportion of *mer* isomer at the expense of both the *u-fac* and *s-fac* isomers is in the direction predicted by Favas and Kepert[17] if the isomer distribution were reflecting that of $Co(dien)^{2+}$ rather than the 3+ complex. Hence, the product distribution is also supportive of electron transfer as the mode of complex formation.

The title complex, then, appears to be generally applicable to a wide variety of synthetic applications. Chromophores of the CoN_6^{3+} type have received the most attention,[4-9] but mixed CoN_4S_2,[10] CoN_4SCl,[11] and CoN_2O_3Cl[18] chromophores can also form rapidly from this precursor. Nonequilibrium isomer distributions are achieved with polyamines, which could lead to unattainable products or products produced in only low yields by more conventional synthetic routes. The complex may also be utilized for mixed-ligand syntheses. We have obtained yields of 20–30% for the (cysteinato)bis(ethylenediamine)cobalt(III) complex[19] by reacting the title complex with a 10% excess of a 1:2 ligand mixture in aqueous solution.

A major advantage in the use of this complex as a synthetic precursor is the rapid complex formation achieved at ambient temperatures with stoichiometric amounts of ligands and/or dilute solutions of ligands. The complex is also soluble in a wide variety of solvents, and synthesis is possible in any of these. The original synthetic procedure of Werner and Feenstra[1] has been improved by two groups.[20,21] We observe little difference in the synthetic utility of the compound prepared by either procedure, indicating that catalytic amounts of Co(II) are present when either method is followed. The solid complex is stable for months on the shelf.[20]

The more commonly used "tris(carbonato)cobaltate(III)" complex is applicable to a wide variety of synthetic applications, but syntheses with this complex usually employ an excess of ligands, and removal of the third carbonato group is often sluggish.[22] Also, strictly nonaqueous preparations with this compound would be difficult since the complex is usually prepared just before use with aqueous hydrogen peroxide.[22]

This study has shown that the mode of rapid complex formation between this complex and ligands is undoubtedly via electron-transfer processes, and previous kinetic studies in this area indicate that the complex is a facile oxidant by either an inner-sphere[14] or an outer-sphere[15] route with many Co(II) complexes. For the inorganic chemist who wishes to employ this complex, the preliminary mechanistic studies reported here suggest two useful experimental notes. First, if a synthesis is being attempted and the reaction is sluggish, a trace of Co^{2+} should speed up the reaction as noted above. Second, if physical solution studies are being made, care should be taken in the choice of buffers employed unless the complex is completely free of Co(II).

Department of Chemistry
University of Miami
Coral Gables, Florida 33124

W. L. Purcell

Received May 27, 1986

(16) Keene, F. R.; Searle, G. H. *Inorg. Chem.* **1974**, *13*, 2173.
(17) Favas, M. C.; Kepert, D. L. *J. Chem. Soc., Dalton Trans.* **1978**, 793.
(18) This work.
(19) Kothari, V. M.; Busch, D. H. *Inorg. Chem.* **1969**, *8*, 2276.
(20) Elgy, C. N.; Wells, C. F. *J. Chem. Soc., Dalton Trans.* **1980**, 2405.
(21) Glerup, J.; Schaffer, C. E.; Springborg, J. *Acta Chem. Scand., Ser. A* **1978**, *A32*, 673.
(22) Shibata, M. *Proc. Jpn. Acad.* **1974**, *50*, 779.

Electronic Control of the Structural Stability of Quasi-Periodic Linear Chains

Sir:

The recent notion of quasi-periodic systems proposed by Steinhardt and colleagues coupled with the observed icosahedral symmetry of electron diffraction patterns in Mn–Al alloys presents systems conceptually intermediate between a random network and the crystalline solid.[1,2] The pentagonal symmetry properties are incommensurate with translational symmetry yet represent a nonrandom arrangement of atoms. What is the electornic nature of such quasi-periodic systems, especially when compared to alternatives, which may or may not possess translational periodicity? In this communication, we shall select a series of linear chains with one orbital per site to model the three cases: periodic, quasi-periodic, and random. We shall analyze the eigenvalue spectra of these model systems and examine their structural stability as a function of electron count.

The model linear chains consist of a single orbital per site. Examples include the π manifold of polyacetylene and the mixed-valence platinum-chain compounds. The energy levels were obtained with use of simple Hückel theory. Since we are interested in energy differences between structures, all the Coulomb integrals α_i are set equal to zero as these parameters only affect the average energy of the band. Also, only nearest-neighbor interactions are included in the model. These Hückel β values will depend on the relevant internuclear separations within the chains.

Four types of linear chains from the three categories were selected as models. For a quasi-periodic system, the chain consists of two basic length scales, L and S, between adjacent atoms arranged in the sequence

SLSSLSLSSLSSL...
(I)

(this scheme represents the sequence of bond lengths within the chain). The motiviation for choosing this type of structure arises from its numerical similarities to the original Penrose tiling.[3] This tessellation fills two-dimensional space using four different shapes and generates a pattern that never repeats itself, i.e. possesses no translational periodicity. In addition, one can find five interpenetrating sets of parallel lines passing through all vertices with spacings in the ratio τ:1 ($\tau \equiv (5^{1/2} + 1)/2 = 1.618\,03...$; the golden mean)[4] and their sequence described by an algorithm using the Fibonacci series. Our "Fibonacci chain" uses the same algorithm with the ratio of the number of S lengths to the number of L lengths for the infinite case also in the ratio τ:1. For internal consistency the remaining chain models are limited to a maximum of two different length scales. We examine two types of translationally periodic chains for comparison with the quasi-periodic system. The first example contains one orbital per unit cell—the well-understood linear chain with equal distances between nearest neighbors.[5] The other example, containing 13 orbitals per unit

(1) Levine, D.; Steinhardt, P. J. *Phys. Rev. Lett.* **1984**, *53*, 2477.
(2) Shechtman, D.; Blech, I.; Gratias, D.; Cahn, J. W. *Phys. Rev. Lett.* **1984**, *53*, 1951.
(3) Penrose, R. *Bull. Inst. Math. Appl.* **1974**, *10*, 266.
(4) Bursill, L. A.; Lin, P. L. *Nature (London)* **1985**, *316*, 50.
(5) Burdett, J. K. *Prog. Solid State Chem.* **1984**, *15*, 173.

0020-1669/86/1325-4069$01.50/0

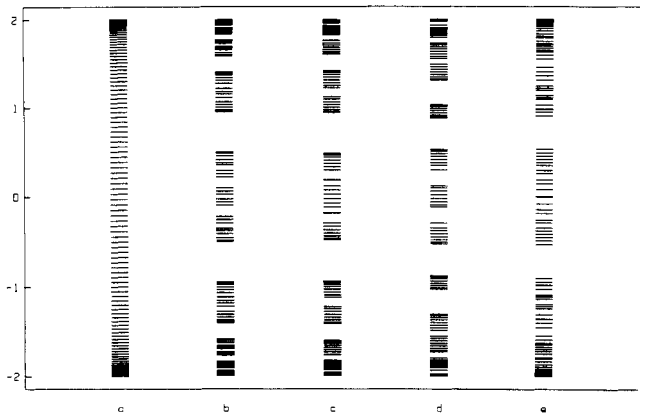

Figure 1. Eigenvalue spectra: (a) periodic chain with a single internuclear distance: (b) Fibonacci chain; (c) 13-atom chain, case II; (d) 13-atom chain, case III; (e) random chain of orbitals. The energy scale is separated in units of β for the periodic chain (a).

cell, has a ratio of the number of S lengths to L lengths equal to 8:5 (=1.6). This is a value close to the ratio τ:1 for the Fibonacci chain. In order to maintain similar local environments of the atoms/orbitals in the Fibonacci and 13-atom chains, we restricted the maximum number of successive S lengths to 2. This condition produces only two distinct types of periodic chains whose bond length sequences are shown by II and III. The final chain model

...SSLSLSSLSLSSL... (II) ...SSLSSLSSLSLSL... (III)

includes a series of randomized arrangements of the length scales that maintains a ratio of S lengths to L lengths equal to the corresponding ratio in the Fibonacci chain as well as limits the number of successive S linkages as for the 13-atom chains. With the description of these chain models in hand, the objectives of this preliminary account include understanding the energetic preference for a given structure as a function of band filling as well as given some insights into their eigenvalue spectra.[6,7]

Before we examine the computational results, three points concerning our method need to be discussed. In the first case, since no analytical forms for the energy bands of the Fibonacci chain or any random system exist to date, the chains were limited to finite length. While the largest chain length studied included 300 orbital sites, we found that ~100 atoms provided sufficient information. Second, to minimize any edge effects from the terminated chains, the first and last members were linked within the Hamiltonian: a Born–von Karman boundary condition.[8] The third point concerns the resonance integrals, β_{ij}, between pairs of orbitals. These terms control the dispersion of the band but not the overall shape of the density of states. In order to compare the total energy for these model systems, we need some constraints on these interaction integrals. The method we selected maintained equal second moments, $\mu_2 = \sum_i E_i^2$, among all systems, which is equivalent to setting the energy fluctuations for the models equal to each other.

In Figure 1 we illustrate the eigenvalue spectra of the representative chains. Certainly the critical observation is the definite series of band gaps appearing in the eigenvalue spectrum of the Fibonacci chain and the fractal nature of the level pattern itself.[9] With respect to the periodic linear chain, the Fibonacci chain and the 13-atom chains will show regions of stability when the Fermi level lies near the band gaps. We also note that the random chain

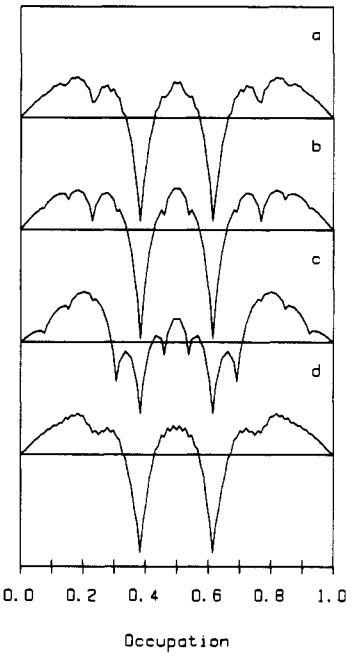

Figure 2. Energy difference as a function of band occupation for the (a) random, (b) 13-atom (case II), (c) 13-atom (case III), and (d) Fibonacci chains with respect to the parent periodic linear chain. The energy separation between adjacent horizontal lines is 1.26β, for β the same as in Figure 1.

contains gaps in its spectrum similar to those of the Fibonacci chain. How can we easily understand these eigenvalues spectra? The translationally periodic 13-atom chains reduce the volume of the first Brillouin zone of the undistorted linear system by a factor of 13, thereby splitting the single band of the parent chain into 13 bands with gaps opening at $|\mathbf{k}| = (\pi/13a), (2\pi/13a), \ldots, (12\pi/13a)$. The integrated DOS (density of states) for each of these bands measures $^1/_{13}$ the total integrated DOS for the parent chain. In addition to this expected pattern, case II exhibits four major band gaps: a consequence of the pseudopentagonal distortion of the parent chain as shown in **1**. For any distortion of

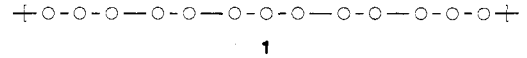

1

the periodic chain that retains translational symmetry, this analysis reproduces the qualitative features of the spectrum, but it is not adequate for the Fibonacci or the random chains.

An alternative approach, which is easily applied to systems without special translational symmetry properties, involves assembling the structure from molecular fragments. For the Fibonacci chain the two length scales L and S are associated with two resonance integrals, β_L and β_S, in the Hamiltonian. Setting β_L to zero initially, we find the chain is composed of trimers and dimers of orbitals whose respective energy levels are well-understood from the solution of the π manifold of the allyl and ethylene units in organic chemistry. In units of β_S, the trimer has energy levels at $-2^{1/2}$, 0, and $+2^{1/2}$ while the dimer has levels at -1 and $+1$.[10] Turning on the β_L interactions broaden these discrete, well-separated levels into bands as shown in Figure 1b. Therefore, we can determine the location of the band gaps for the Fibonacci chain by counting the number of trimers and dimers in the chain. For the infinite case, the ratio of the number of trimers to dimers is τ:1. The integrated DOS for the five primary bands have the following relative magnitudes with increasing energy: τ, 1, τ, 1, and τ. The largest gaps occur at the band occupation of $(\tau + 1)/(3\tau + 2) = 2 - \tau$ (=0.381 96...) and $\tau - 1 = 1 - (2 - \tau)$ (=0.618 03...), at which we anticipate the greatest stabilization with respect to the linear chain. Since these argu-

(6) More rigorous mathematical treatments of solutions to the Schrödinger equation with nearly periodic potentials are found in: (a) Kohmoto, M.; Kadanoff, L.; Tang, C. *Phys. Rev. Lett.* **1983**, *50*, 1870. (b) Ostlund, S.; Pandit, R.; Rand, D.; Schnellnhuber, H.; Siggia, E. *Phys. Rev. Lett.* **1983**, *50*, 1873. (c) Ostlund, S.; Pandit, R. *Phys. Rev. B: Condens. Matter* **1984**, *29*, 1394.

(7) Odagaki, T.; Nguyen, D. *Phys. Rev. B: Condens. Matter* **1986**, *33*, 2184.

(8) Ashcroft, N. W.; Mermin, N. D. *Solid State Physics*; Saunders College: Philadephia, 1976.

(9) Kadanoff, L., private communication.

(10) Albright, T. A.; Burdett, J. K.; Whangbo, M.-H. *Orbital Interactions in Chemistry*; Wiley: New York, 1985.

ments apply to the other models as well, one can only comment on the gross features of the integrated DOS.

Before examining the structural stabilities, we also mention an alternative segmentation of the Fibonacci chain. From the opposite extreme, we can set β_S to zero, which produces a chain of dimers (interaction integrals β_L) and isolated atoms. Upon introduction of the β_S interaction, the initial "three-level" diagram expands to an eigenvalue spectrum with characteristics similar to those of Figure 1b. This viewpoint has some similarities to the soliton model in polymers.

We can depict the regions of stabilization for the various structural models by displaying the energy difference curves as a function of band filling. Figure 2 shows these curves with the periodic linear chain as the reference. The alternative structure has the lower total energy when the curve drops below $\Delta E = 0$. As predicted from its eigenvalue spectrum, the Fibonacci chain is clearly more stable than the present chain for the fractional band occupations, 0.382 and 0.618 ($2 - \tau$ and $\tau - 1$, respectively). However, by nature of the structure of the periodic alternative, case II, this chain and Fibonacci model are essentially isoenergetic. The other periodic example III is not favored at these occupancies since the intrinsic connectivity is different: the dimers lie adjacent to each other. The random models never become the energetic preferences at the crucial occupancies of 0.382 or 0.618. Thus, the Fibonacci chain possesses some intrinsic symmetry property that at certain electron counts favors it geometrical configuration over any random arrangement of orbitals. The important result of our calculation, placing the Fibonacci chain isoenergetic with a translationally periodic one (albeit with a rather large lattice constant) allows direct comment on the feasilibility of observing more examples of such species. The arrangement is clearly not a metastable curiosity but one that can energetically compete with periodic alternatives. It is in fact more stable[11] than the simplest periodic chain of five atoms per cell with dimers and trimers.

We may view these energy difference curves using the language of moments. Energy difference curves as a function of electron count between the structural possibilities often have a characteristic shape determined by the order of the first disparate moment, $\mu_n(\rho)$, of their energy density of states.[12] The energy difference curves for both the Fibonacci chain and the 13-atom chains are dominated by contributions from the fourth- and sixth-moment differences. Since the nth moment of a network is directly related to the number of walks of length n beginning and ending at the same site, the qualitative similarities between the Fibonacci chain and the 13-atom chains derive from their essential connectivities. A detailed enumeration of the walks to second- and third-nearest neighbors, which we will report elsewhere,[11] indicate the subtle differences between the two chains. The Fibonacci chain has smaller fourth and smaller sixth moments than any random arrangement of L- and S-length scales with the same ratio.

With a single orbital per site we are exclusively examining the effects of the intrinsic connectivity properties on the energy spectrum, and so our results will apply to many one-dimensional solids. Chemically realistic examples include polyacetylene, square-planar-coordinated platinum chains, and many of the organic metals involving planar organic units. The results suggest that under sufficient oxidation or reduction conditions, a quasi-periodic configuration for these one-dimensional systems is a possible reaction product. Note, however, that in order to achieve these critical band occupations for one-dimensional materials dopant concentrations exceeding 20% are necessary. Examining two- and three-dimensional systems is an obvious extension of this analysis, as well as coloring the chains with different atomic species. Although known only for alloy systems at present, can we anticipate the possibility of one-dimensional materials exhibiting quasi-crystalline states?

Acknowledgment. This research was supported by the National Science Foundation via NSF Grants DMR 8414175 and DMR 8216892 and the Dow Chemical Co. We are grateful to Leo Kadanoff and Leo Falicov for useful conversations.

Department of Chemistry
University of Chicago
Chicago, Illinois 60637

Jeremy K. Burdett*
Gordon J. Miller

Received June 2, 1986

(11) Burdett, J. K.; Miller, G. J., to be submitted for publication.
(12) (a) Ducastelle, F.; Cyrot-Lackmann, F. *J. Phys. Chem. Solids* **1971**, *32*, 285. (b) Burdett, J. K.; Lee, S. *J. Am. Chem. Soc.* **1985**, *107*, 3050.

Bromine Atom Abstraction from Aryl and Alkyl Bromides by the Triplet Excited State of the Tetrakis(μ-pyrophosphito)diplatinum(II) Tetraanion

Sir:

The tetrakis(μ-pyrophosphito)diplatinum(II) tetraanion, $Pt_2(\mu\text{-}P_2O_5H_2)_4^{4-}$ has recently been the subject of several photochemical studies because of its having a long-lived phosphorescence at ambient temperature in aqueous solution.[1] This triplet excited state is both a strong reductant and oxidant.[2] Under photochemical conditions ($\lambda_{max} > 350$ nm), we have recently found that the excited state reacts with alkyl and aryl bromides.[3] For bromobenzene, the product complex $Pt_2(\mu\text{-}P_2O_5H_2)_4(C_6H_5)Br^{4-}$ is that resulting from an oxidative addition reaction. For both bromopentafluorobenzene and 1,2-dibromoethane,[4] however, the final product is $Pt_2(\mu\text{-}P_2O_5H_2)_4Br_2^{4-}$. It has previously been suggested that the mechanism of these reactions with alkyl and aryl halides involves an $S_{RN}1$ pathway with $Pt_2(\mu\text{-}P_2O_5H_2)_4^{4-*}$ as reductant. This $S_{RN}1$ pathway is a stepwise electron-transfer mechanism leading to the formation of bromide ion and an aryl or alkyl radical.[5] We have used transient difference spectroscopy to investigate the photochemical reaction of $Pt_2(\mu\text{-}P_2O_5H_2)_4^{4-}$ with C_6H_5Br, C_6F_5Br, and 1,2-$C_2H_4Br_2$. In all three cases the first detectable photoproduct is $Pt_2(\mu\text{-}P_2O_5H_2)_4Br^{4-}$. This mixed-valence Pt(II)Pt(III) intermediate shows a characteristic absorption band at 340 nm ($\epsilon = 5 \times 10^4$ L mol^{-1} cm^{-1}) (Figure 1).[6] We have confirmed this assignment by separately synthesizing $Pt_2(\mu\text{-}P_2O_5H_2)_4Br^{4-}$ by carrying out the biphotonic photoionization of $Pt_2(\mu\text{-}P_2O_5H_2)_4^{4-}$ in the presence of excess bromide ion (eq 1).[7]

$$Pt_2(\mu\text{-}P_2O_5H_2)_4^{4-} + Br^- \xrightarrow{2h\nu} Pt_2(\mu\text{-}P_2O_5H_2)_4Br^{4-} + e(H_2O)^- \quad (1)$$

Laser (Nd–YAG at 355 nm) photolysis of aqueous methanolic solutions of $K_4[Pt_2(\mu\text{-}P_2O_5H_2)_4]$ containing either C_6H_5Br, C_6F_5Br,

(1) Sperline, R. P.; Dickson, M. K.; Roundhill, D. W. *J. Chem. Soc., Chem. Commun.* **1977**, 62–63.
(2) Che, C.-M.; Butler, L. G.; gray, H. B. *J. Am. Chem. Soc.* **1981**, *103*, 7796–7797. Heuer, W. B.; Totten, M. D.; Rodman, G. S.; Hebert, E. J.; Tracy, H. K.; Nagle, J. K. *J. Am. Chem. Soc.* **1984**, *106*, 1163–1164. Peterson, J. R.; Kalyanasundaram, K. *J. Phys. Chem.* **1985**, *89*, 2486–2492.
(3) Roundhill, D. M. *J. Am. Chem. Soc.* **1985**, *107*, 4253–4254.
(4) Marshall, J. L.; Stiegman, A. E.; Gray, H. B.; *ACS Symp. Ser.* **1986**, *307*, 166–176.
(5) Kochi, J. *Organometallic Mechanisms and Catalysis*; Academic: New York, 1978, Chapter 7. Rossi, R. A.; de Rossi, R. H. *Aromatic Substitution by the $S_{RN}1$ Mechanism*; ACS Monograph 178; *American Chemical Society*: Washington, DC, 1983.
(6) This extinction coefficient has been estimated from the ratio of the changes in optical density at 340 and 368 nm. The respective triplet state quenching rates for $Pt_2(\mu\text{-}P_2O_5H_2)_4^{4-*}$ with C_6H_5Br, C_6F_5Br, and 1,2-$C_2H_4Br_2$ in aqueous methanol are 1×10^5, 2×10^7 and 8×10^6 M^{-1} s^{-1}. These rate data were obtained from Stern–Vollmer plots.
(7) Cho, K. C.; Che, C.-M. *Chem. Phys. Lett.* **1986**, *124*, 313–316. Roundhill, D. M.; Atherton, S. J. *J. Am. Chem. Soc.*, in press. $Pt_2(\mu\text{-}P_2O_5H_2)_4Br^{4-}$ has also been prepared by the pulse radiolysis of aqueous solutions of $Pt_2(\mu\text{-}P_2O_5H_2)_4Br_2^{4-}$ (Che, C.-M.; Gray, H. B.; Atherton, S. J.; Lee, W.-M., submitted for publication). In this work λ_{max} is observed at 370 nm. The difference in peak maxima arises because in our laser photolysis experiment we cannot subtract the contribution from the bleached band at 368 nm. In our uncorrected spectra, overlapping affects the observed peak maximum position of the absorption band of interest.

0020-1669/86/1325-4071$01.50/0